Applied Catalysis A: General 486 (2014) 69–76

Contents lists available at ScienceDirect

Applied Catalysis A: General

journal homepage: www.elsevier.com/locate/apcata

Synthesis of cyclic carbonate from carbon dioxide and epoxides with polystyrene-supported quaternized ammonium salt catalysts

Sun-Do Lee[a], Bo-Mi Kim[b], Dong-Woo Kim[b], Moon-Il Kim[b], Kuruppathparambil Roshith Roshan[b], Min-Kyung Kim[c], Yong-Son Won[c], Dae-Won Park[b,*]

[a] Zeus Oil and Chemicals Co. Ltd., Busan 617-805, Republic of Korea
[b] School of Chemical and Biomolecular Engineering, Pusan National University, Busan 609-735, Republic of Korea
[c] Department of Chemical Engineering, Pukyung National University, Busan 608-739, Republic of Korea

ARTICLE INFO

Article history:
Received 17 July 2014
Received in revised form 14 August 2014
Accepted 22 August 2014
Available online 29 August 2014

Keywords:
Polystyrene
Quaternization
Ionic liquid
Epoxide
Carbon dioxide

ABSTRACT

Polystyrene-supported quaternized ammonium salt catalysts (PS-alkyl-AX) were synthesized and characterized by various physicochemical analytic methods such as EA, FT-IR, XPS, and SEM. The reactivity of the catalysts was investigated for the synthesis of allyl glycidyl carbonate from CO_2 and allyl glycidyl ether under mild reaction conditions. The PS-alkyl-AX catalysts showed good catalytic activity without using any solvent due to the synergistic effect of NH functional group and quaternary ammonium salt structure. Theoretical studies using density functional theory (DFT) was applied to investigate the reaction mechanism. The PS-hexyl-MeI catalyst was readily recoverable and reusable in subsequent reaction cycles without a significant loss in its activity.

1. Introduction

Although CO_2 is thermodynamically stable, its desirable physical properties such as nontoxicity and nonflammability, along with its ready abundance, have attracted researchers to employ it as an environmentally friendly substitute for harmful chemicals such as phosgene and carbon monoxide, in the interest of environmental preservation and better resource utilization [1–5].

Thus, the chemical fixation of CO_2 owing to its low cost is a field of interesting research with multiple objectives such as reducing the atmospheric CO_2 concentration and synthesizing industrially important chemicals. In this context, the reaction of CO_2 with epoxides as an atom-efficient synthesis of cyclic carbonates is a dynamic field of interest.

Five-membered cyclic carbonates are industrially valuable chemicals widely employed as aprotic solvents, electrolytes in lithium-ion batteries, monomer units of polycarbonates, and so on [6,7]. Their challenging synthesis has led to the development of an appreciable number of catalyst systems, including room-temperature and task-specific ionic liquids (ILs), metal complexes of salen and porphyrins, organometallic catalysts, quaternary ammonium salts, organic bases, and immobilized catalysts [7–22].

The immobilization of a catalyst and reagents on a variety of polymeric supports is attracting considerable attention as "green chemistry" in both industrial and laboratory chemical processes because of the ease of handling and recycling and the unique microenvironment formed by the reactants within the polymeric support [23–25]. Recently, polymer-supported ILs have been exploited as heterogeneous catalysts in the synthesis of cyclic carbonates and were found to offer the dual features of a homogeneous IL and a heterogeneous catalyst. Compared to pure ILs, such heterogeneous catalysts have additional advantages such as a reduction in the amount of ILs employed, recovery of the catalyst from the reaction mixture, and ease of separation [26–28].

Divinylbenzene (DVB) cross-linked polystyrene is one of the most useful polymers owing to its compatibility with a wide range of reaction conditions. Furthermore, because of its simple preparation, recyclability, environmental stability, low cost, and nonsolubility in commonly used organic solvents and water, DVB cross-linked polystyrene has attracted much attention as an efficient heterogeneous catalyst support [28–31].

In our previous work [32], we immobilized the imidazolium salt IL onto the Merrifield resin by alkoxylation with bromoalcohol followed by quaternization with methylimidazole.

* Corresponding author. Tel.: +82 51 510 2399; fax: +82 51 512 8563.
E-mail address: dwpark@pusan.ac.kr (D.-W. Park).

http://dx.doi.org/10.1016/j.apcata.2014.08.029
0926-860X/

In this study, different polystyrene-supported quaternary ammonium salts were prepared by the reaction of PS and alkyl diamine followed by quaternization with an alkyl halide, with varying chain lengths of the alkyl diamine and different cation and anion of the alkyl halide. The performance of these catalysts in the synthesis of cyclic carbonate from allyl glycidyl ether (AGE) and CO_2 was investigated. These catalysts containing NH– group between the PS and quaternized ammonium group, can activate the epoxide ring, and therefore, showed better catalytic performance compared to the PS-supported quaternary ammonium salts without NH– group in the linker [33]. For a better understanding of the reaction mechanism, DFT studies were performed. The effects of the catalyst structure, CO_2 pressure, and reaction temperature were also discussed. A recyclability test of the catalyst was carried out to assess the stability of this catalyst system.

2. Experimental

2.1. Synthetic scheme

The synthesis of the quaternized ammonium salt anchored to PS was carried out via two steps as shown in Fig. S1 (Supporting Information). First, a mixture of PS (Merrifield peptide resin, Aldrich, 1% DVB, 4.5 mmol Cl/g) and acetonitrile was stirred for 12 h at 25 °C, then alkylene diamine was added with KOH, and this mixture was stirred for 48 h at 80 °C to yield alkylenediamine-anchored PS (PS-*alkyl*-diamine). The second step is the quaternization of the PS-*alkyl*-diamine to form PS-*alkyl*-AX by its reaction with an alkyl halide for 72 h at 50 °C. The precipitate was filtered and washed with ethanol and then dried in a vacuum oven for 12 h at 60 °C to prepare PS-*alkyl*-AX.

2.2. Characterization of the catalyst

Elemental analysis (EA) was carried out using Vario EL III. The samples (2 mg) were heated to 1100 °C, and sulfanilic acid was used as a standard. Fourier transform infrared (FT-IR) spectra were obtained on an AVATAR 370 Thermo Nicolet spectrophotometer with a resolution of 4 cm^{-1}. XPS analyses were performed using an X-ray photoelectron spectrometer (VG, ESCALAB 250) with monochromatic Al Kα radiation ($h\nu$ = 1486.6 eV). The surface morphology was observed using an S-4200 field emission scanning electron microscope (FE-SEM, Hitachi-3500N).

2.3. Synthesis of AGC from AGE and CO_2

Allyl glycidyl carbonate (AGC) was synthesized by the coupling reaction of AGE and CO_2 in the presence of PS-*alkyl*-AX. All the reactions were carried out in a 60-mL stainless-steel batch reactor with a magnetic stirrer at 600 rpm. In a typical batch reaction, a predetermined amount of catalyst was charged into the reactor containing 52.3 mmol of AGE. The reaction was carried out under a constant pressure of CO_2 at different temperatures. After the completion of the reaction, the reactor was cooled to 0 °C, and the products were identified by gas chromatography (Agilent HP 6890 A) with a capillary column (HP-5, 30 m × 0.25 μm) using a flame ionized detector. The product yield was determined using an internal standard method with biphenyl (0.05 g) as the standard.

3. Results and discussion

3.1. Characterization of the catalysts

The organic compositions of PS, PS-*alkyl*-diamine, and PS-*alkyl*-AX were determined by elemental analysis (EA), and the results are summarized in Table 1. The increase in the amount of nitrogen from PS to PS-*alkyl*-diamine indicated that the Cl of the DVB cross-linked chloromethylated polystyrene reacted with the NH_2 of the alkyldiamine to form N—C bonds and eliminate HCl during covalent anchoring to the polystyrene resin. The amount of PS-*alkyl*-QA immobilized on the polystyrene support varied from 2.0 to 2.7 mmol/g-cat.

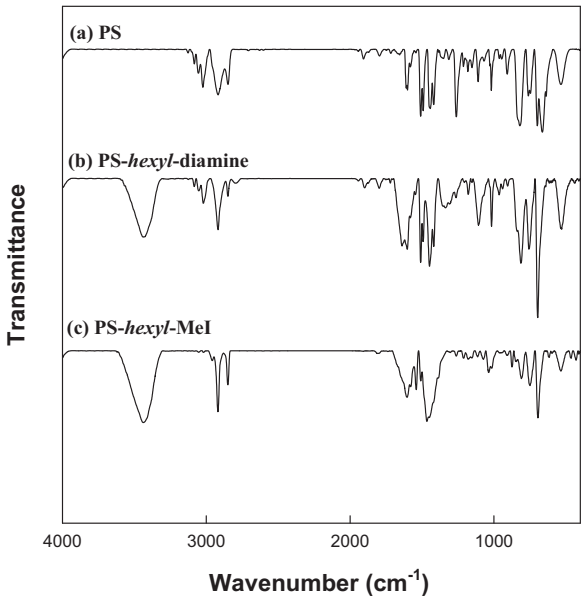

Fig. 1. FT-IR spectra of (a) PS, (b) PS-*hexyl*-diamine and (c) PS-*hexyl*-MeI.

The successful immobilization of the quaternary ammonium salt on the surface of the polystyrene support was confirmed using FT-IR spectroscopy (Fig. 1). In the FT-IR spectral analyses of PS-*hexyl*-diamine, PS-*hexyl*-MeI, and MPR, the characteristic peak corresponding to the stretching frequency of the CH_2Cl functional group (1265 cm^{-1}) disappeared in the spectra of PS-*hexyl*-diamine and PS-*hexyl*-MeI, suggesting the complete modification of MPR [26–28]. New peaks were observed for PS-*hexyl*-MeI in the regions 1560–1650 and 3400 cm^{-1}, which were absent from the MPR spectrum; these peaks are associated with the NH– bending and stretching frequencies [34].

Further corroboration of the successful quaternization under microwave irradiation was provided through XPS analyses. The N 1s spectra of PS-*hexyl*-diamine and PS-*hexyl*-MeI are presented in Fig. 2. While PS-*hexyl*-diamine (Fig. 2b) showed a sole characteristic amine nitrogen 1s peak at 399.4 eV, the quaternized species (PS-*hexyl*-MeI; Fig. 2a) exhibited one additional peak centered at 402.4 eV, which is consistent with the literature data for the 1s binding energy of quaternized nitrogen ($-N^+Me_3$) species. This observation could be rationalized by the fact that the exposed amine groups of PS-*hexyl*-diamine indeed underwent a successful quaternization. The new peak (402.4 eV) observed in the characteristic region for the nitrogen atom provided conclusive evidence for the successful quaternization of PS-*hexyl*-diamine [35–37]. Moreover, the I 3d spectra of PS-*hexyl*-MeI were acquired to identify the bonding nature of the halogen associated with the metal species, as illustrated in Fig. S2. The I 3d peak was observed at 619.6 eV in the case of PS-*hexyl*-MeI, which indicated the anionic state of iodine [38,39]. The aforementioned results are a clear indication of the successful immobilization of the quaternized ammonium salt on the support, as shown in Fig. S1.

The SEM images of PS, PS-*alkyl*-diamine, and PS-*alkyl*-MeI are presented in Fig. 3. The images show that the diameter of the

Table 1
Elemental analysis results of PS-*alkyl*-MeI.

	CHN from elemental analysis			Amount of anion species on IL (mmol/g)
	N (wt%)	C (wt%)	H (wt%)	
PS-CH_2Cl	0	77.7	6.5	–
PS-*ethyl*-diamine	6.9	79.8	8.0	–
PS-*ethyl*-MeI	4.3	62.4	7.2	2.0
PS-*butyl*-diamine	7.0	79.2	8.1	–
PS-*butyl*-MeI	4.2	58.2	6.5	2.4
PS-*hexyl*-diamine	7.0	79.7	8.0	–
PS-*hexyl*-MeI	4.3	55.3	6.1	2.7

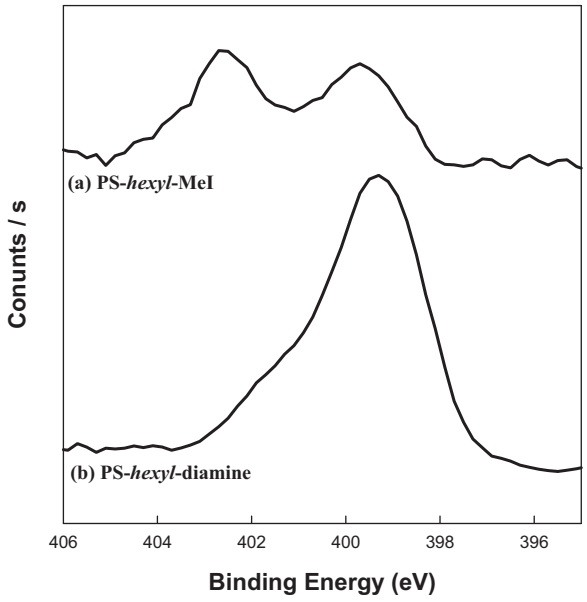

Fig. 2. N 1s XPS spectra of (a) PS-*hexyl*-MeI and (b) PS-*hexyl*-diamine.

polymer beads was approximately 70–80 μm and the spherical shape of the beads was retained even after immobilization.

3.2. Synthesis of AGC from AGE and CO_2

3.2.1. Effect of the catalyst structure

The activity of the various catalysts was tested at 120 °C and an initial CO_2 pressure of 1.2 MPa in a batch autoclave reactor using the reaction of AGE and CO_2 to produce AGC, and the results are summarized in Table 2. The activity of the catalysts depends strongly on the structure of the immobilized quaternary salt active sites on the PS support. Nearly no product was detected without the quaternary ammonium functional group. PS-*alkyl*-diamine showed no conversion of AGE. However, PS-*alkyl*-MeI showed higher than 91% yield of AGC. The yield of AGC increased slightly when the alkyl chain length of the alkyldiamine increased from ethyl to butyl to hexyl.

The effect of the counteranion to the quaternary ammonium halide was very significant. The yield of AGC for PS-*hexyl*-MeX

Table 2
Effects of the structure of PS-*alkyl*-AX on the reactivity for the synthesis of AGC.

Catalyst	Conversion (%)	Selectivity (%)	Yield (%)
PS-*ethyl*-diamine	0	–	–
PS-*ethyl*-MeI	91.5	99.9	91.5
PS-*butyl*-MeI	91.8	99.9	91.8
PS-*hexyl*-MeI	92.8	99.9	92.8
PS-*hexyl*-BuCl	28.3	99.9	28.3
PS-*hexyl*-BuBr	60.2	99.9	60.2
PS-*hexyl*-BuI	95.3	99.9	95.3
PS-*hexyl*-EtI	93.2	99.9	93.2
PS-*hexyl*-HeI	98.3	99.9	98.3

Reaction condition: Catalyst = 0.6 mol%, Temperature = 120 °C, Initial CO_2 pressure = 1.2 MPa, Reaction time = 4 h.

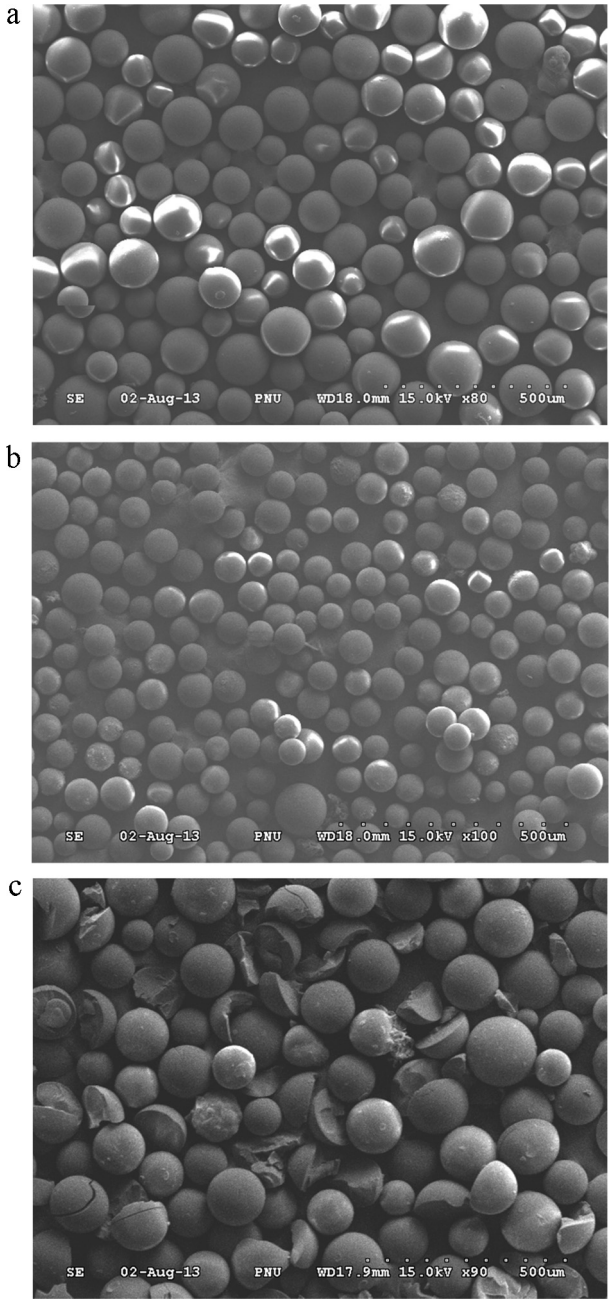

Fig. 3. SEM images of (a) PS, (b) PS-*hexyl*-diamine and (c) PS-*hexyl*-MeI.

increased in the following order: PS-*hexyl*-BuCl (28.3%) < -BuBr (60.2%) < -BuI (95.3%), which corresponds to the increasing nucleophilicity of the halide anion: $Cl^- < Br^- < I^-$. According to the mechanism proposed in previous works [14,40,41], the nucleophilic attack of the halide anion on the epoxide ring is the rate-determining step, and its leaving ability in the ring-closing step is very important for the five-membered cyclic carbonate synthesis.

The effect of the alkyl chain length of the alkyl halide on the AGC synthesis was also investigated (Table 2). For the PS-*hexyl*-AI catalysts, the yield of AGC increased in the order -MeI (92.8%) < -EtI (93.2%) < -BuI (95.3%) < -HexI (98.3%). Indeed, the bulkiness of quaternary ammonium ions forces the iodide away from the quaternary alkyl ammonium cation. Therefore, the activity of the quaternary salt increased with the size of the alkyl cation.

3.2.2. Effect of reaction conditions

The effect of the CO_2 pressure on the catalytic activity of PS-*hexyl*-MeI was studied at 120 °C under an initial pressure range 0.6–2.5 MPa (total pressure of AGE and CO_2), and the results are shown in Table 3. The AGC yield increased with pressure in the range 0.6–2.0 MPa. However, the yield decreased at high pressure (2.5 MPa). This can be explained qualitatively by the effect of pressure on the concentration of CO_2 and epoxide in the two phases in the reaction system [42]. The upper phase is the vapor phase, and the bottom phase is the liquid phase. The reaction took place mainly in the liquid phase because the catalyst was dispersed in the liquid phase. When the pressure was higher than 2.5 MPa, the CO_2 concentration was too high and inhibited the contact of AGE with the catalyst by a dilution effect [43]. Song et al. [42] reported the dominant role of the solvent power of CO_2 to extract epoxide at high CO_2 pressure in the cycloaddition of CO_2 and propylene oxide (PO).

When the reaction of CO_2 and AGE was carried out at a constant pressure of 0.6 MPa in a semi-batch reactor using a back-pressure regulator, the AGC yield was 93.9%, much higher than that using a batch reactor (59.1%). This is because the high CO_2 pressure can be maintained with a continuous supply of CO_2 as long as the CO_2 was consumed by the cycloaddition reaction.

The effect of reaction time on the AGC yield is shown in Fig. 4. The reaction was conducted at 120 °C and 1.2 MPa of total initial pressure. The yield of AGC increased with increasing reaction time up to 6 h. Extended reaction times of 8–12 h did not appear to have further effects on the activity; hence, a reaction time of 6 h was chosen to be optimum.

The effect of the reaction temperature on the cycloaddition reaction was studied with PS-*hexyl*-MeI at 1.2 MPa of total pressure under batch operation, and the results are shown in Table 4. The AGC yield increased on increasing the temperature from 80 to 140 °C; however, it decreased at 160 °C, probably because of the formation of AGE oligomers and some by-products such as 3-allyloxy-1,2-propanediol.

Fig. 5 shows the effect of the catalyst concentration on the cycloaddition of CO_2 and AGE catalyzed by PS-*hexyl*-MeI at 120 °C and 1.2 MPa of total pressure. The yield of AGC increased with

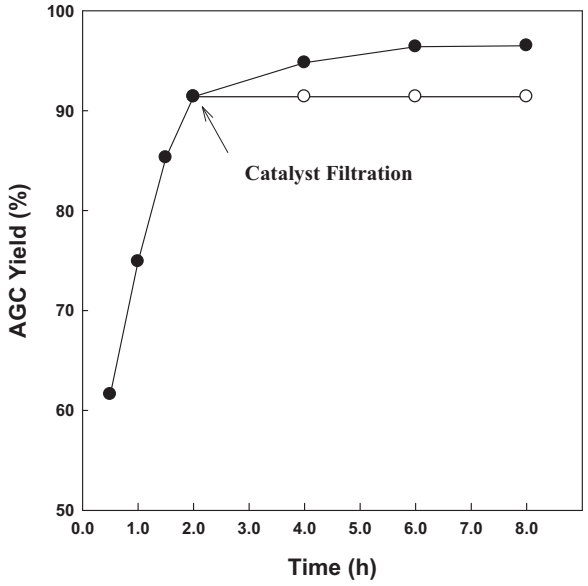

Fig. 4. Effect of reaction time on the yield of AGC (Reaction condition: Catalyst = 6 mol% PS-*hexyl*-MeI, Temp. = 120 °C, Initial CO_2 pressure = 1.2 MPa).

Table 3
Effects of CO_2 pressure on the reactivity for the synthesis of AGC.

Pressure (MPa)	Conversion (%)	Selectivity (%)	Yield (%)
0.6	59.1	99.9	59.1
0.6[a]	95.3	98.6	93.9
0.8	84.5	99.9	84.5
1.0	85.6	99.9	85.6
1.2	92.8	99.9	92.8
1.4	95.9	99.9	95.9
2.0	97.9	99.9	97.9
2.5	98.1	95.6	93.7

Reaction condition: Catalyst = PS-*hexyl*-MeI 0.6 mol%, Temperature = 120 °C, Reaction time = 4 h.
[a] Semibatch operation under constant pressure.

Table 4
Effects of reaction temperature on the reactivity for the synthesis of AGC.

Temperature (°C)	Conversion (%)	Selectivity (%)	Yield (%)
80	33.3	99.9	33.3
100	84.1	99.9	84.1
120	92.8	99.9	92.8
140	94.5	99.9	94.5
160	92.3	98.1	90.5

Reaction condition: Catalyst = PS-*hexyl*-MeI 0.6 mol%, Initial CO_2 pressure = 1.2 MPa, Reaction time = 4 h.

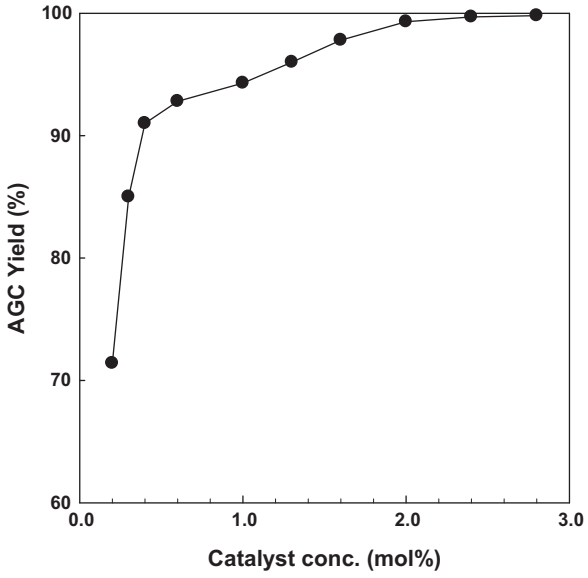

Fig. 5. Effects of catalyst concentration on the yield of AGC (Reaction condition: Catalyst = PS-*hexyl*-MeI, Temp. = 120 °C, Initial CO_2 pressure = 1.2 MPa).

Table 5
Yield of cyclic carbonates for the cycloaddition of CO_2 and various epoxides with PS-*hexyl*-MeI catalyst.

Epoxides	Product	Time (h)	Yield (%)
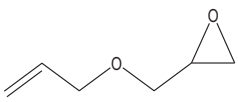	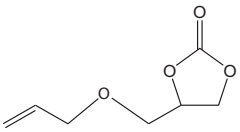	6	97.9
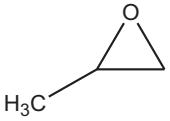	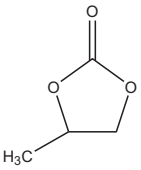	6	98.3
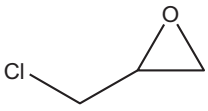	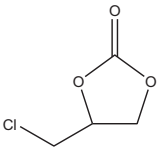	6	96.2
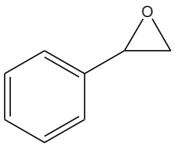	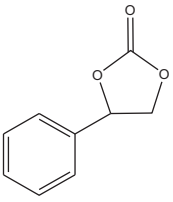	12	96.7
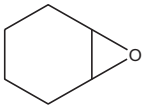	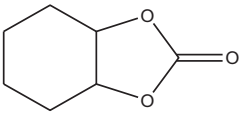	24	65.3

Reaction condition: Catalyst = PS-*hexyl*-MeI 0.6 mol%, Temp. = 120 °C, Initial CO_2 pressure = 1.2 MPa, Reaction time = 4 h, Reaction time = 6–24 h.

increasing catalyst amount and approached 100% when using more than 2 mol% catalyst.

3.2.3. Reaction with other epoxides

The cycloaddition of CO_2 with other epoxides catalyzed by PS-*hexyl*-MeI was also tested at 120 °C and 1.2 MPa of total pressure, and the results are summarized in Table 5. The catalyst could effectively convert all the epoxides studied to the corresponding cyclic carbonates under relatively mild conditions without the use of any solvent or cocatalyst. However, cyclohexene oxide showed a much lower yield because of steric hindrance [44].

3.2.4. Recyclability test

The stability of the PS-*hexyl*-MeI catalyst was evaluated in recycling experiments. For each cycle, the used catalyst was separated by filtration, washed with methanol to remove the products adhering to the surface of the catalyst, dried at room temperature, and then reused directly for the next run without regeneration. The activity of the reused PS-*hexyl*-MeI catalyst is summarized in Table 6. Although the conversion of AGE decreased slightly with the catalyst over three cycles, the selectivity toward GC was almost the same as that achieved with the fresh catalyst. To determine whether the active center of PS-*hexyl*-MeI underwent any leaching from the immobilized polystyrene, FT-IR analyses of the fresh PS-*hexyl*-MeI catalyst and that used for three cycles were performed (Fig. 6). The characteristic peaks of PS-*hexyl*-MeI were similar for the recycled and fresh catalysts. The XPS spectra of fresh

Table 6
Recycling tests of PS-*hexyl*-MeI.

Recycle	Conversion (%)	Selectivity (%)	Yield (%)
Fresh	92.8	99.9	92.8
1	92.2	99.9	92.2
2	91.0	99.9	91.0
3	90.0	99.9	90.0
4	87.2	99.9	87.2

Reaction condition: Catalyst = PS-*hexyl*-MeI 0.6 mol%, Temp. = 120 °C, Initial CO_2 pressure = 1.2 MPa, Reaction time = 4 h.

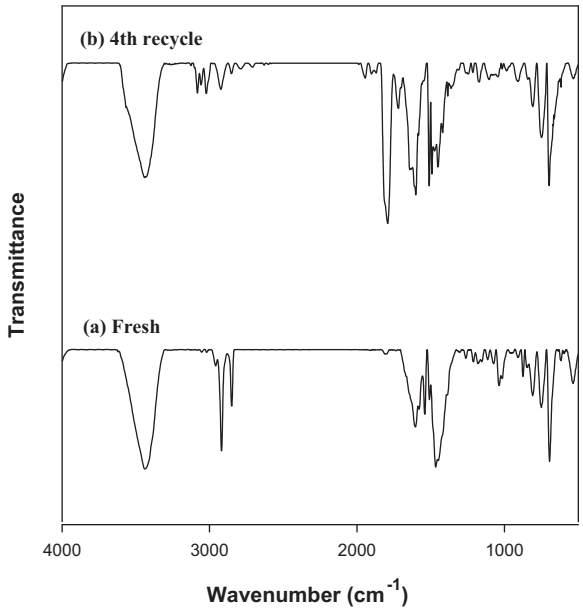

Fig. 6. FT-IR spectra of (a) fresh and (b) reused PS-*hexyl*-MeI.

PS-*hexyl*-MeI and that after three cycles (Fig. 7) demonstrated similar spectra. The peak at 401.7 eV corresponding to the quaternary ammonium nitrogen and those of I^- remained intact, even though the intensities decreased slightly. Therefore, it can be concluded that the PS-*hexyl*-MeI catalyst could be recycled up to three

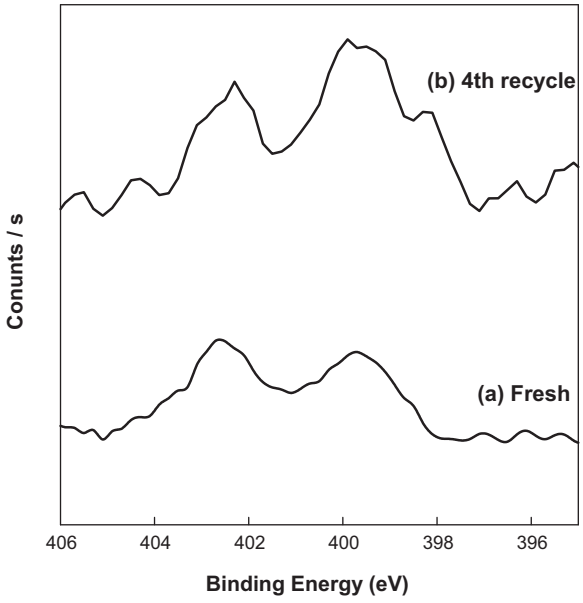

Fig. 7. N 1s XPS spectra of (a) fresh and (b) reused PS-*hexyl*-MeI.

Table 7
Effects of TBAI co-catalyst on the reactivity for the synthesis of AGC.

Catalyst	Co-catalyst	Conversion (%)	Selectivity (%)	Yield (%)
–	TBAI	75.8	93.7	71.0
PS-*hexyl*-diamine	–	0	–	–
PS-*hexyl*-MeI	–	92.8	99.9	92.8
PS-*hexyl*-diamine	TBAI	79.4	93.6	74.3
PS-*hexyl*-MeI	TBAI	98.4	97.9	96.3

Reaction condition: Catalyst = PS-*hexyl*-diamine or PS-*hexyl*-MeI = 0.6 mol%, TBAI (tetrabutylammonium iodide) = 0.6 mol%, Temperature = 120 °C, Initial CO_2 pressure = 1.2 MPa, Reaction time = 4 h.

consecutive cycles without any considerable loss of its initial activity. In order to check the possible contribution of homogeneous catalytic activity of active PS-*hexyl*-MeI leached into solution, a hot catalyst filtration test was performed after 3 h of reaction. The AGC yield in the filtrate did not decrease after the catalyst was removed while maintaining the reaction temperature constant, indicating that the catalysis was not due to the soluble homogeneous species (Fig. 4).

3.2.5. Effect of the cocatalyst

The effect of a cocatalyst, tetrabutylammonium iodide (TBAI), on the activity of PS-*hexyl*-MeI was studied at 120 °C and 1.2 MPa of total pressure (Table 7). PS-*hexyl*-diamine alone showed no catalytic activity for the cycloaddition of AGE and CO_2. TBAI can activate the reaction as a homogeneous catalyst, and showed 71.0% AGC yield. When TBAI was used with PS-*hexyl*-diamine, the mixed catalyst exhibited a slightly higher AGC yield (74.3%) than with TBAI alone. PS-*hexyl*-MeI showed the highest AGC yield of 92.8% because it has quaternized ammonium salt active sites anchored to PS in one body. TBAI also increased AGC yield of PS-*hexyl*-MeI.

3.2.6. DFT generated reaction mechanism with the PS-alkyl-AX catalyst

Density functional theory (DFT) has been now widely applied for gathering theoretical insights about the whereabouts of the mechanism involved in catalysis. A handful of reports have made it clear that, the hydrogen bonding groups along with the halide anions in the catalyst system plays synergistically for an accelerated synthesis of cyclic carbonates from CO_2 and epoxides [45–49]. Hence, herein we conducted DFT calculations with Gaussian 09 set package with B3LYP correlation functional, where the basis sets employed were the 6-311++ G (d,p) for non-iodine atoms, and the LANL2DZ dp for iodine. For the sake of simplicity, propylene oxide (PO) and a model PS-alkyl-AX (Fig. 8) catalyst which has similar molecular features as that of the employed catalysts were subjected to the theoretical simulations. The series of events as obtained from these simulations are portrayed in Fig. 8.

In the first step, the 'O' atom of the epoxide binds to the catalyst moiety via hydrogen atom of the NH group of PS-alkyl-MeI catalyst and an intermediate-1 (Int-1) is formed (see Fig. 8b). At this juncture, the bond distance between the epoxide 'O' atom and the 'H' atom of NH group is 1.97 Å which is a typical hydrogen bond length, whereby the bond strength of the βC—O of the epoxide weakens (Int-1, Fig. 8b). The O–CH_2 bond of the PO subsequently breaks as the proton becomes increasingly closer to the epoxide oxygen, in which the bond distance now became 1.06 Å in transition state-1 (TS-1, Fig. 8c). By the time the Int-2 forms, the proton from the 'N' atom detaches completely and the hydroxy derivative of the ring opened epoxide appears along with the new C-I covalent bond with a length of 2.19 Å (Fig. 8d). As the CO_2 enters the catalytic loop, the proton starts reverting back to the nitrogen atom of the catalyst (as shown by the decrease in N-H bond length), generating a net negative charge on the "O" atom of the ring opened epoxide (TS-2, Fig. 8e). This oxy anion makes a nucleophilic attack on the carbon atom of CO_2, and deforms its linear geometry. Subsequently, a carbonate complex was found as a result of the above step (Int-3, Fig. 8f) and then the C—I bond weakens as displayed by an increase in bond length from 2.2 to 2.99 resulting in a net positive charge on the βC of epoxide (TS-3, Fig. 8g). In the last step, the carbonate complex attacks the βC and cycloaddition completes, regenerating the PS-alkyl-AX catalyst (product complex, Fig. 8h).

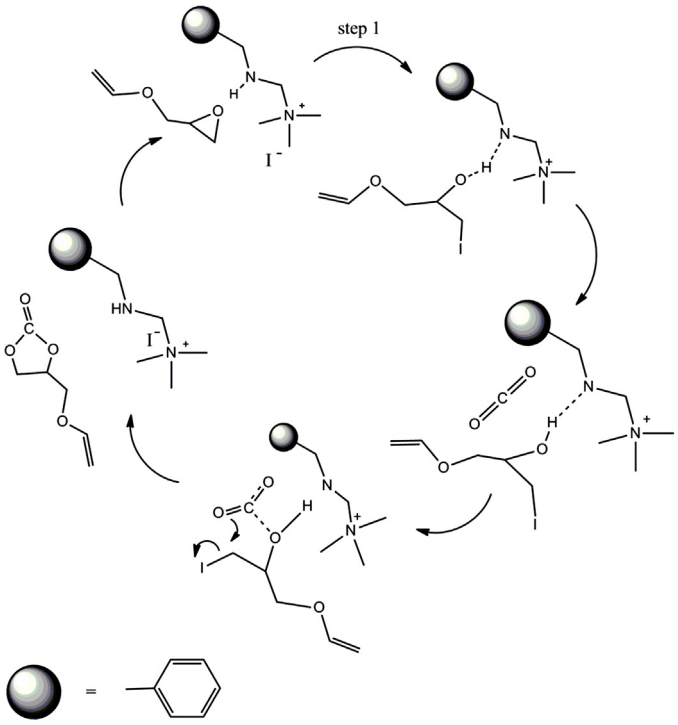

Scheme 1. A plausible mechanism of AGC synthesis from AGE-CO_2 coupling based on the experimental and DFT results.

Hence, putting together the experimental and DFT results with the earlier reports [25,31,34], led us to a plausible mechanism (Scheme 1) for the PS-*hexyl*-MeI-catalyzed cycloaddition of CO_2 with AGE to afford AGC. The AGE molecules approach PS-hexyl-MeI, and gets tethered to the NH group of the catalyst via hydrogen bonding through the epoxy "O' atom resulting in the polarization of the C—O bond; the site of attack is configured in a way such that the nucleophilic anion of the immobilized quaternary ammonium salt is able to initiate an attack on the least hindered (β) carbon atom of the epoxide ring. Ring opening of the epoxide occurs, followed by the formation of a new C—X covalent bond. Following, the proton returns to the nitrogen atom generating an oxy anion. CO_2 was attacked by this oxyanion, thereby activating the otherwise stable linear molecule. An alkyl carbonate anion complex is formed as a result of this, which eventually yields AGC upon subsequent ring closure and catalyst regeneration.

As seen in Scheme 1, hydrogen bonding is the key chemical interaction in the operation that holds the epoxide in the proper orientation to facilitate an effective nucleophilic attack by the halide anion. Hence, the improved activity of this PS-*alkyl*-AX catalyst system over previously reported homogeneous quaternary salt catalysts could be attributed to the increased accessibility of the NH groups toward epoxide coordination and the greater CO_2 diffusivity made possible by the cross-linked PS support.

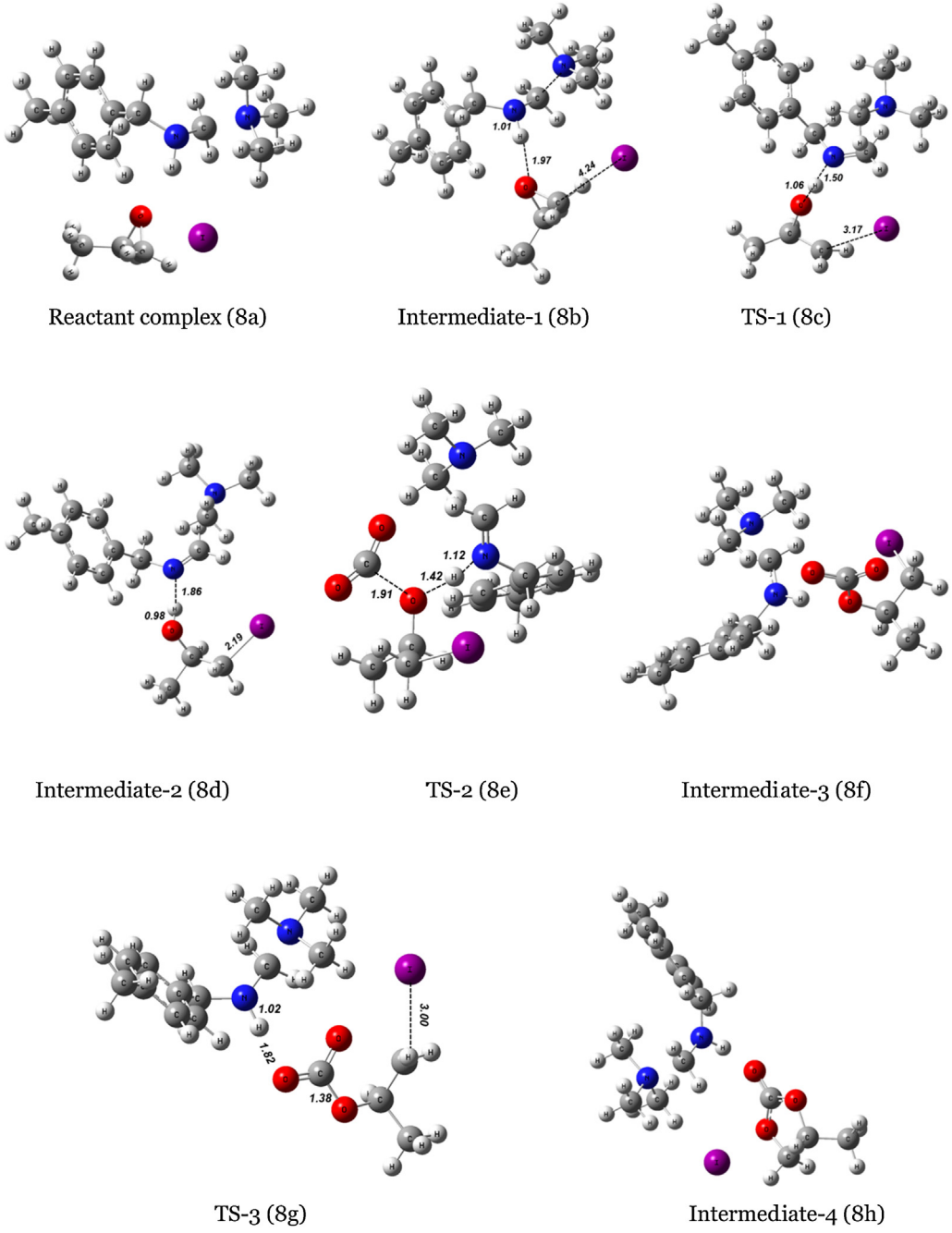

Fig. 8. Gauss view images of the simulated intermediates and transition states of PS-*alkyl*-MeI catalyzed cycloaddition of propylene oxide with CO_2.

4. Conclusions

Various polystyrene-supported quaternized ammonium salt catalysts were prepared, and their molecular and structural compositions were characterized through FT-IR, XPS, SEM, and elemental analyses. The PS-alkyl-AXs were found to catalyze the cycloaddition of CO_2 with AGE under mild reaction conditions (0.6 mol% catalyst loading, 120 °C, 1.2 MPa CO_2) to 98% completion with 99% propylene carbonate selectivity. The explicit role of the NH functional group in the catalysis was closely investigated by using parameter studies and DFT calculations; the results obtained affirmed the possibility of an interaction between the NH– group and the epoxide oxygen. The PS-*alkyl*-AXs were found to efficiently catalyze the cycloaddition of aliphatic and aromatic terminal epoxides with excellent selectivity, and they could be reused more than three times without any significant loss of activity.

Acknowledgements

This work was supported by the National Research Foundation of Korea (NRF Global Frontier Program 2013M3A6B1078877). The authors are also grateful to Research Institute of Industrial Technology of Pusan National University.

Appendix A. Supplementary data

Supplementary data associated with this article can be found, in the online version, at http://dx.doi.org/10.1016/j.apcata.2014.08.029.

References

[1] M. Aresta, A. Dibenedetto, Dalton Trans. 28 (2007) 2975–2992.

[2] M. North, R. Pasquale, C. Young, Green Chem. 12 (2010) 1514–1539.
[3] T. Sakakura, J.C. Choi, H. Yasuda, Chem. Rev. 107 (2007) 2365–2387.
[4] K.M. Kerry Yu, I. Curcic, J. Gabriel, S.C.E. Tsang, ChemSusChem 1 (2008) 893–899.
[5] M. Mikkelsen, M. Jørgensen, F.C. Krebs, Energy Environ. Sci. 3 (2010) 43–81.
[6] A.-A.G Shaikh, S. Sivaram, Chem. Rev. 96 (1996) 951–976.
[7] T. Sakakura, K. Kohno, Chem. Commun. 11 (2009) 1312–1330.
[8] J. Sun, L. Han, W. Cheng, J. Wang, X. Zhang, S. Zhang, ChemSusChem 4 (2011) 502–507.
[9] T. Ema, Y. Miyazaki, S. Koyama, Y. Yano, T. Sakai, Chem. Commun. 48 (2012) 4489–4491.
[10] A. Coletti, C.J. Whiteoak, V. Conte, A.W. Kleij, ChemCatChem 4 (2012) 1190–1196.
[11] S. Liang, H. Liu, T. Jiang, J. Song, G. Yang, B. Han, Chem. Commun. 47 (2011) 2131–2133.
[12] W.-L. Dai, L. Chen, S.F. Yin, W.H. Li, Y.-Y. Zhang, S.L. Luo, C.T. Au, Catal. Lett. 137 (2010) 74–80.
[13] L. Han, S.W. Park, D.W. Park, Energy Environ. Sci. 2 (2009) 1286–1292.
[14] J. Ma, J. Liu, Z. Zhang, B. Han, Green Chem. 14 (2012) 2410–2420.
[15] L. Han, H.J. Choi, S.J. Choi, B. Liu, D.-W. Park, Green Chem. 13 (2011) 1023–1028.
[16] M.M. Dharman, H.J. Choi, D.W. Kim, D.W. Park, Catal. Today 164 (2011) 544–547.
[17] K.R. Roshan, G. Mathai, J. Kim, J. Tharun, G.-A. Park, D.-W. Park, Green Chem. 14 (2012) 2933–2940.
[18] J. Sun, J. Wang, W. Cheng, J. Zhang, X. Li, S. Zhang, Y. She, Green Chem. 14 (2012) 654–660.
[19] A.C. Kathalikkattil, J. Tharun, R. Roshan, H.-G. Soek, D.-W. Park, Appl. Catal. A 447–448 (2012) 107–114.
[20] D.W. Kim, R. Roshan, J. Tharun, A. Cherian, D.W. Park, Korean J. Chem. Eng. 30 (2013) 1973–1984.
[21] Y. Du, F. Cai, D.L. Kong, L.N. He, Green Chem. 7 (2005) 518–523.
[22] Q. He, J.W. O'Brien, K.A. Kitselman, L.E. Tompkins, G.C.T. Curtis, F.M. Kerton, Catal. Sci. Technol. 4 (2014) 1513–1528.
[23] N.E. Leadbeater, M. Marco, Chem. Rev. 102 (2002) 3217–3274.
[24] C.A. McNamara, M.J. Dixon, M. Bradley, Chem. Rev. 102 (2002) 3275–3300.
[25] S. Bhattacharyya, Com. Chem. High Throughput Screen 3 (2000) 65–92.
[26] G.R. Krishnan, K. Sreekumar, Appl. Catal. A: Gel. 353 (2009) 80–86.
[27] J. Sun, W. Cheng, W. Fan, Y. Wang, Z. Meng, S. Zhang, Catal. Today 148 (2009) 361–367.
[28] C. Qi, J. Ye, W. Zang, H. Jiang, Adv. Synth. Catal. 352 (2010) 1925–1933.
[29] G. Roshinkar, S. Kamble, A. Kumbhar, R. Salunkhe, Catal. Commun. 12 (2011) 1442–1447.
[30] Y. Xie, Z. Zhang, T. Jiang, J. He, B. Han, T. Wu, K. Ding, Angew. Chem. 119 (2007) 7393–7396.
[31] Q.W. Song, L.N. He, J.Q. Wang, H. Yasuda, T. Sakakura, Green Chem. 15 (2013) 110–115.
[32] J.I. Yu, H.J. Choi, M. Selvaraj, D.W. Park, React. Kinet. Mech. Catal. 102 (2011) 353–365.
[33] Y.Y. Zhang, L. Chen, S.F. Yin, S.L. Luo, C.T. Au, Catal. Lett. 142 (2012) 1376–1381.
[34] A. Chowdhury, S.T. Thynell, Thermochim. Acta 443 (2006) 159–172.
[35] J. Tharun, Y. Hwang, R. Roshan, S. Ahn, A.C. Kathalikkattil, D.-W. Park, Catal. Sci. Technol. 2 (2012) 1674–1680.
[36] J. Tharun, D.W. Kim, R. Roshan, Y. Hwang, D.-W. Park, Catal. Commun. 31 (2013) 62–65.
[37] S. Eyley, W. Thielemans, Chem. Commun. 47 (2011) 4177–4179.
[38] D. Derouet, S. Forgeard, J.C. Brosse, J. Emery, J.Y. Buzare, J. Polym. Sci. Pol. Chem. 36 (1998) 437–453.
[39] B. Yu, F. Zhou, C. Wang, W. Liu, Eur. Poly. J. 43 (2007) 2699–2707.
[40] Y. Zhao, J.-S. Tian, X.-H. Qi, Z.-N. Han, Y.-Yi. Zhuang, L.-N. He, J. Mol. Catal. A: Chem. 271 (2007) 284–289.
[41] F. Castro-Gomez, G. Salassa, A.W. Kleij, C. Bo, Chem. Eur. J. 19 (2013) 6289–6298.
[42] J. Song, Z. Zhang, S. Hu, T. Wu, T. Jiang, B. Han, Green Chem. 11 (2009) 1031–1036.
[43] D.J. Darensbourg, R.M. Mackiewicz, D.R. Billodeaux, Organometallics 24 (2005) 144–148.
[44] C.J. Whiteoak, N. Kielland, V. Laserna, E.C. Escudero-Adan, E. Martin, A.W. Kleij, J. Am. Chem. Soc. 135 (2013) 1228–1231.
[45] J. Tharun, G. Mathai, A.C. Kathalikkattil, R. Roshan, B. Kim, D.W. Park, Phys. Chem. Chem. Phys. 15 (2013) 9029–9033.
[46] J. Tharun, G. Mathai, A.C. Kathalikkattil, R. Roshan, J.Y. Kwak, D.W. Park, Green Chem. 15 (2013) 1673–1677.
[47] K.R. Roshan, A.C. Kathalikkattil, J. Tharun, D.W. Kim, Y.S. Won, D.W. Park, Dalton Trans. 43 (2014) 2023–2031.
[48] A.C. Kathalikkattil, R. Roshan, J. Tharun, H.G. Seok, H.S. Ryu, D.W. Park, ChemCatChem 6 (2014) 284–292.
[49] A.C. Kathalikkattil, D.W. Kim, J. Tharun, H.G. Seok, R. Roshan, D.W. Park, Green Chem. 16 (2014) 1607–1616.